SANDIA REPORT

SAND2004-8037
Unlimited Release
Printed January 2004

Nanoscale Hotspots Due to Nonequilibrium Thermal Transport

S. Sinha, K.E. Goodson

Prepared by
Sandia National Laboratories
Albuquerque, New Mexico 87185 and Livermore, California 94550

Sandia is a multiprogram laboratory operated by Sandia Corporation,
a Lockheed Martin Company, for the United States Department of Energy's
National Nuclear Security Administration under Contract DE-AC04-94AL85000.

Approved for public release; further dissemination unlimited.

Sandia National Laboratories

Issued by Sandia National Laboratories, operated for the United States Department of Energy by Sandia Corporation.

NOTICE: This report was prepared as an account of work sponsored by an agency of the United States Government. Neither the United States Government, nor any agency thereof, nor any of their employees, nor any of their contractors, subcontractors, or their employees, make any warranty, express or implied, or assume any legal liability or responsibility for the accuracy, completeness, or usefulness of any information, apparatus, product, or process disclosed, or represent that its use would not infringe privately owned rights. Reference herein to any specific commercial product, process, or service by trade name, trademark, manufacturer, or otherwise, does not necessarily constitute or imply its endorsement, recommendation, or favoring by the United States Government, any agency thereof, or any of their contractors or subcontractors. The views and opinions expressed herein do not necessarily state or reflect those of the United States Government, any agency thereof, or any of their contractors.

Printed in the United States of America. This report has been reproduced directly from the best available copy.

Available to DOE and DOE contractors from
U.S. Department of Energy
Office of Scientific and Technical Information
P.O. Box 62
Oak Ridge, TN 37831

Telephone: (865) 576-8401
Facsimile: (865) 576-5728
E-Mail: reports@adonis.osti.gov
Online ordering: http://www.doe.gov/bridge

Available to the public from
U.S. Department of Commerce
National Technical Information Service
5285 Port Royal Rd
Springfield, VA 22161

Telephone: (800) 553-6847
Facsimile: (703) 605-6900
E-Mail: orders@ntis.fedworld.gov
Online order: http://www.ntis.gov/help/ordermethods.asp?loc=7-4-0#online

SAND2004-8037
Unlimited Release
Printed January 2004

Nanoscale Hotspots Due to Nonequilibrium Thermal Transport

Sanjiv Sinha, K. E. Goodson,
Department of Mechanical Engineering (Thermosciences Division), Stanford University

Abstract

Recent experimental and modeling efforts have been directed towards the issue of temperature localization and hotspot formation in the vicinity of nanoscale heat generating devices. The nonequilibrium transport conditions which develop around these nanoscale devices results in elevated temperatures near the heat source which can not be predicted by continuum diffusion theory. Efforts to determine the severity of this temperature localization phenomena in silicon devices near and above room temperature are of technological importance to the development of microelectronics and other nanotechnologies. In this work, we have developed a new modeling tool in order to explore the magnitude of the additional thermal resistance which forms around nanoscale hotspots from temperatures of 100 – 1000K. The models are based on a two fluid approximation in which thermal energy is transferred between "stationary" optical phonons and fast propagating acoustic phonon modes. The results of the model have shown excellent agreement with experimental results of localized hotspots in silicon at lower temperatures. The model predicts that the effect of added thermal resistance due to the nonequilibrium phonon distribution is greatest at lower temperatures, but is maintained out to temperatures of 1000K. The resistance predicted by the numerical code can be easily integrated with continuum models in order to predict the temperature distribution around nanoscale heat sources with improved accuracy.

Additional research efforts also focused on the measurements of the thermal resistance of silicon thin films at higher temperatures, with a focus on polycrystalline silicon. This work was intended to provide much needed experimental data on the thermal transport properties for micro and nanoscale devices built with this material. Initial experiments have shown that the exposure of polycrystalline silicon to high temperatures may induce recrystallization and radically increase the thermal transport properties at room temperature. In addition, the defect density was observed to play a major role in the rate of change in thermal resistivity as a function of temperature.

Acknowledgement

This work was conducted as a part of Sandia National Laboratories Campus Executive Laboratory Directed Research and Development (LDRD) program. The authors wish to recognize former Sandian Samuel Graham, Jr. for his programmatic leadership in this endeavor, and Sandia's Executive Vice President Joan Woodard for her sponsorship.

Contents

I. Introduction

Recent research has shown that the temperature rise near nanoscale semiconductor devices can yield dramatically larger temperatures than those predicted using continuum diffusion theory. This phenomena has been experimentally demonstrated in micron-scale doped silicon resistors at low temperatures. In order to explain the size scale and temperature range over which this phenomena is important, as well as the magnitude, additional modeling and experiments are necessary.

The research efforts this year worked to develop theory for heat conduction from an electronically generated optical phonon hotspot. The approach is to avoid atomistic or particle based numerical models, and focus on providing corrections to continuum diffusion theory which is normally used in existing hydrodynamic electron transport models. The analytical subcontinuum thermal model developed here predicts reduced phonon conduction from the nanoscale optical phonon hotspot and is found to compare well with experimental data. A key challenge of this analysis is the large departure from equilibrium of phonon states within a variety of energy ranges and branches. This is addressed by defining separate temperatures for stationary and propagating phonons. This two-fluid approximation for phonons simplifies the phonon dispersion such that energy moments of the Boltzmann equation yield coupled but simplified equations for the two phonon fluids. Another key assumption is the use of a single overall scattering time, which enables the simplification of the collision integral to yield a closed-form thermal resistance between the temperature of phonons transporting heat and an average phonon temperature. This two-fluid resistance is a sub-continuum correction to the resistance calculated from diffusion theory and can be readily incorporated in hydrodynamic models. This results in a calculated resistance of the heat transfer from a stationary reservoir of optical phonons to the acoustic mode which results in an additional resistance above that predicted by continuum diffusion theory.

In our work, we model the thermal transport and the formation of nanoscale heat sources using two methods: 1) Atomistic Modeling and 2) Two-fluid phonon transport models. The atomistic modeling work explores the transport and decay of key optical phonons at the hotspot through atomistic simulations. The objective is to estimate scattering rates that can be used to predict temperature rise in the transistor using previously developed compact models. The hotspot size and energy is based on Monte Carlo device simulations. The simulations show that an optical phonon hotspot is associated with a local strain that stabilizes it. The decay of the hotspot is brought about by the cancellation of this strain. This work helps in elucidating important phonon physics for thermal simulations of devices.

In the two fluid-phonon model, we compare the model predictions with experimental data in single crystal silicon. The data show excellent agreement between model and experimental results. Additional comparisons of the thermal resistance of ballistic phonon transport near a spherical hotspot in bulk silicon with the two-fluid resistance model were also explored in this work. The two-fluid resistance provides the impedance due to strong excitation of a stationary phonon mode and the ballistic resistance provides the impedance due to emission of propagating phonons from the hotspot. The two-fluid resistance is found to be larger than the resistance due to ballistic emission by a factor of more than 20 for a hotspot of radius 10 nm at room temperature. This is partly due to the severe assumption about the nature of phonon excitation inherent in the two-fluid model. The cumulative resistance is about 850 times larger than the resistance calculated from the diffusion theory. This factor decreases to around 30 as temperature in bulk

silicon as temperature is increased from 300K to 1000K. Thus, the resulting two-fluid thermal resistance is dominant when the hotspot is small compared to the acoustic phonon mean free path and over most applicable temperature ranges for nanoscale transistors. The resistance predicted here serves as a correction term for predicting the temperature rise in a transistor using continuum diffusion theory. The two-fluid model developed here is intended as a starting point for exploring the problem of phonon transport in nanotransistors where sub-continuum phenomena will be stronger due to reduced size scale dimensions.

II. Atomistic Simulations of Non-equilibrium Phonons in Nanotransistors

II.a. Introduction

With the advent of sub-100 *nm* transistors around the corner, the problem of localized heating of the silicon lattice, induced by electron relaxation, is of increased importance. Nanoscale heat sources or phonon hotspots, with characteristic dimensions of the order of 20*nm* and energy density reaching $10^{18} W/m^3$, are expected to form in the drain of such devices as shown in Figure 1. The disparity in the electron and phonon relaxation rates by almost an order of magnitude, causes significant non-equilibrium in the phonon system. This work focuses on the sub-continuum conduction of heat from such sources, in thermal environments that closely resemble silicon transistors.

We have shown through thermometry measurements on a silicon film that temperatures near such a sub-continuum heat source are severely underestimated by the diffusion theory of heat conduction [1], which is widely used in industrial device simulators. We have developed a compact model for predicting the peak temperature inside such a source that agrees well with the experimental data [2]. The model predicts a fourfold increase in the drain resistance due to this effect for a channel length smaller than 30 nm [3]. The phonon transport problem in a realistic device geometry is however far more complex. A numerical solution to the phonon Boltzmann transport equation (BTE) can be obtained through Monte Carlo [4] or finite-volume quadrature based [5] methods. However, a crucial input to all such BTE solutions is the enharmonic phonon scattering rate. Though theoretical constructs for evaluating phonon-phonon and phonon-impurity scattering rates were developed nearly fifty years ago [6], they are extremely difficult to evaluate in practice. Instead, simplified expressions obtained from perturbation theory [7] are usually fitted to thermal conductivity data to yield material specific scattering rates. Since the contribution of optical phonons to the thermal conductivity is negligible near room temperatures for most semiconductors, their scattering rates have remained largely unexplored except for direct band gap materials used in optoelectronics, where optical phonons play a significant role [8].

In this work, we approach this problem of estimating optical phonon decay rates through atomistic simulations. We create phonon wavepackets with size, energy density, polarization and wavevector that resemble expected hotspots in a silicon device. The evolution of such wavepackets is studied in a one-dimensional system. The scattering rates obtained from this study are intended to be embedded in Monte Carlo phonon simulations and/or compact BTE models. These can then be employed to investigate actual device geometries. This will significantly improve the state of art in device thermal simulations to keep in pace with shrinking device size.

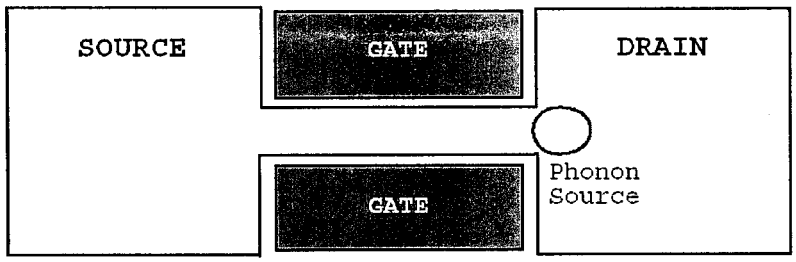

Fig. 1. Schematic of an ultra-thin body SOI nanotransistor showing the location of the high density phonon source or hotspot in the drain. The characteristic dimension is around $20nm$ with a peak power density of the order of $10^{18}W/m^3$

II.b. Creating the Hotspot

From electron-phonon scattering theory, primarily two types of phonons are generated in silicon devices: the f and g-phonons [9]. In this study we focus on the g-type longitudinal optical phonon. The Stillinger-Weber [10] potential for silicon is used to calculate the phonon eigenmodes of the bulk lattice. A linear combination of the modes is used to create a wavepacket centered in wavevector space at 0.3 of the Brillouin zone edge along the <100> direction. This represents the g-phonon generated by electron relaxation in a device. The size and energy are adjusted to yield the desired hotspot. Figure 2 shows the lattice displacements that comprise the wavepacket and Figure 3 shows the energy distribution in space. For computational feasibility, a one dimensional system is chosen that has a square cross-section comprising 4×4 lattice cells and is nearly a micron long.

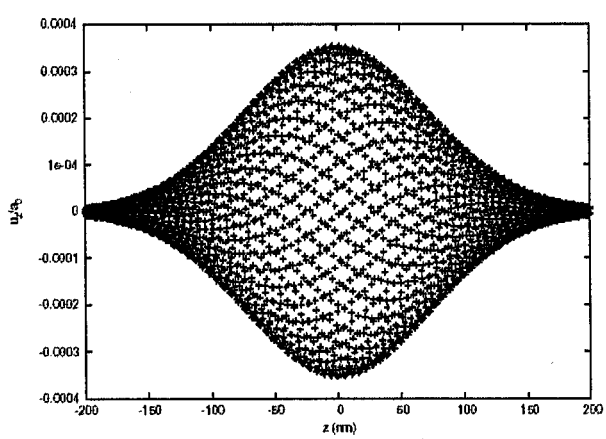

Fig. 2. A localized phonon source or hotspot is created from a linear combination of the lattice vibrational modes, centered to have the required wavevector and polarization. The longitudinal displacements of individual atoms at different axial locations are shown in the figure.

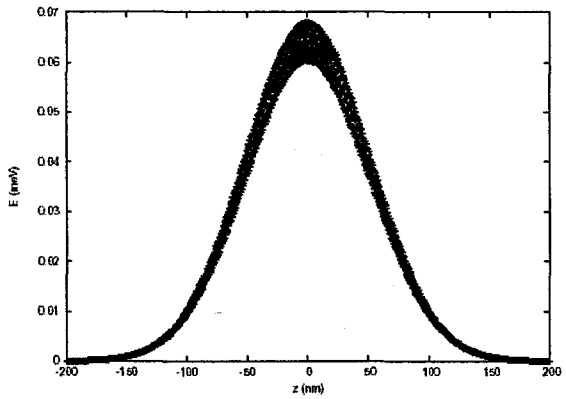

Fig. 3. The energy distribution for a typical hotspot is shown. The total energy in this case is 1 *meV*

II.c. Modecular Dynamics Simulations

The phonon wavepacket representing the hotspot is embedded in the one-dimensional silicon box (shown in Figure 4) at the start of molecular dynamics (MD) simulations. Since the wavepacket travels at nearly 10^3 *m/s*, we need to use periodic boundary conditions to track the wavepacket for times of the order of nanoseconds. As explained later, this is also found to cause unwanted interference effects. Constant energy molecular dynamic simulations are performed to evolve the system in time. Approximately 6 days of computer time on 16 nodes of a cluster are needed to get 5 ns of data. Post processing involves decomposing the lattice displacements into the eigenmodes to separate optical and acoustic phonons in the system. This is a fairly expensive step taking almost as much computer time as the MD part.

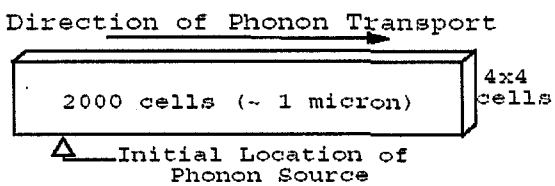

Fig. 4. The simulation is performed for a one dimensional silicon tube with 64000 atoms and dimensions as indicated above. The hotspot is placed on the left and its time evolution is studied through molecular dynamics.

II.d. Simulation Results

The evolution of the wavepacket is shown in Figure 5. The displacements associated with longitudinal optical modes are shown on the left in each snapshot. To the right are the displacements associated with longitudinal acoustic modes. The wavepacket shown has 1 *eV* of energy and a width of 300*nm*. Placing the hotspot in the otherwise undisturbed lattice creates a localized strain immediately. A negative strain field is also created outside the hotspot to counteract this local strain at the hotspot. We believe that while the local strain is physically realistic, the strain field is an artifact of the finite system size. The simulations indicate that the local strain is key to the stability of the optical wavepacket. The "decay" of the optical hotspot is actually brought about when the local positive strain is canceled due to interference from the strain field. One way to get around this problem is to pause the MD simulations after a few steps

and introduce extra strain in the system to cancel out the strain field. We believe this will stabilize the original wavepacket and allow us to observe physically realistic scattering. We are currently investigating this approach.

Ultimately we are interested in determining the temperature rise in the transistor. In our earlier work [2], we found that the peak temperature rise at the hotspot is approximately given by

$$\Delta T = \frac{1}{C}\int \dot{n}_G \tau_p \hbar\omega g(\omega) d\omega \qquad (1)$$

where C is the heat capacity, $\dot{n}_G$ is the phonon generation rate, τp is the phonon decay rate and $g(\omega)$ is the phonon density of states. An approximate frequency independent acoustic phonon scattering rate had been used in the past work, leading to the following expression,

$$\Delta T = \frac{\dot{q}\,\tau}{C} \qquad (2)$$

where $\dot{q}$ is the peak volumetric power generation. With the availability of key phonon decay rates, Equation 1 can be used in preference to the simplistic estimate of Equation 2.

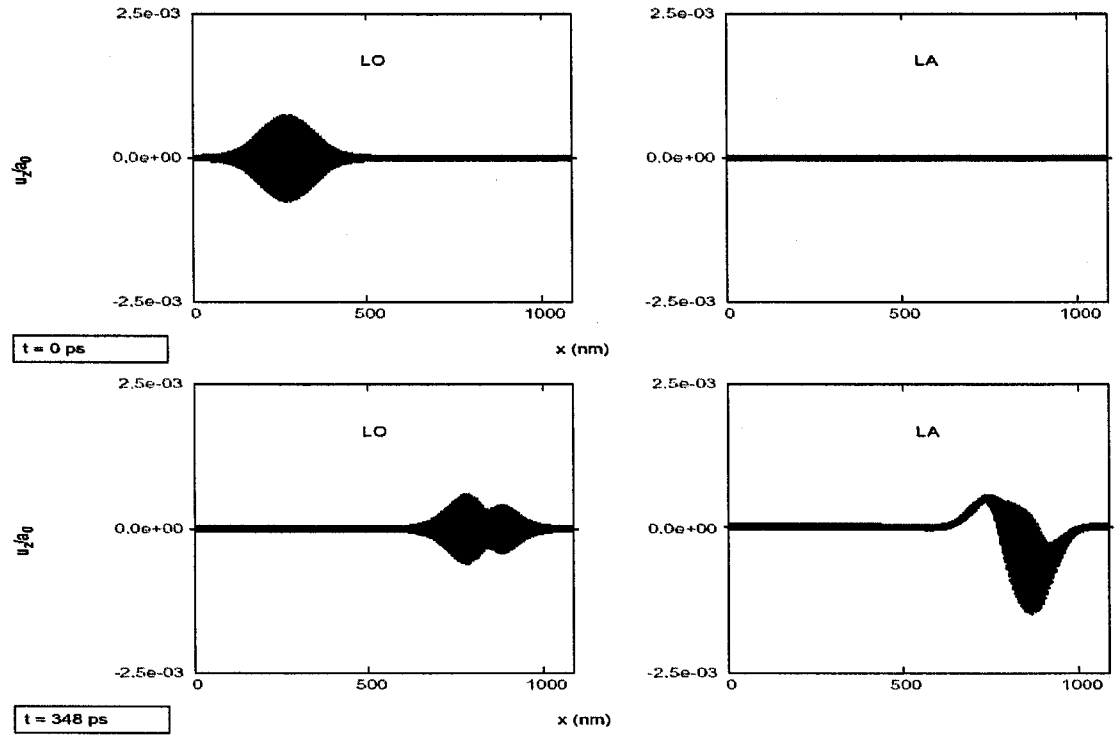

Fig. 5. The time evolution of a 1 *eV* optical phonon hotspot is shown. At t = 0 only longitudinal optical (LO) modes are present in the system. These constitute a localized phonon source similar to that in a transistor. The second snapshot at t = 348 *ps* shows the decay of the optical modes in the hotspot triggered by the cancellation of the local strain by the rest of the strain field.

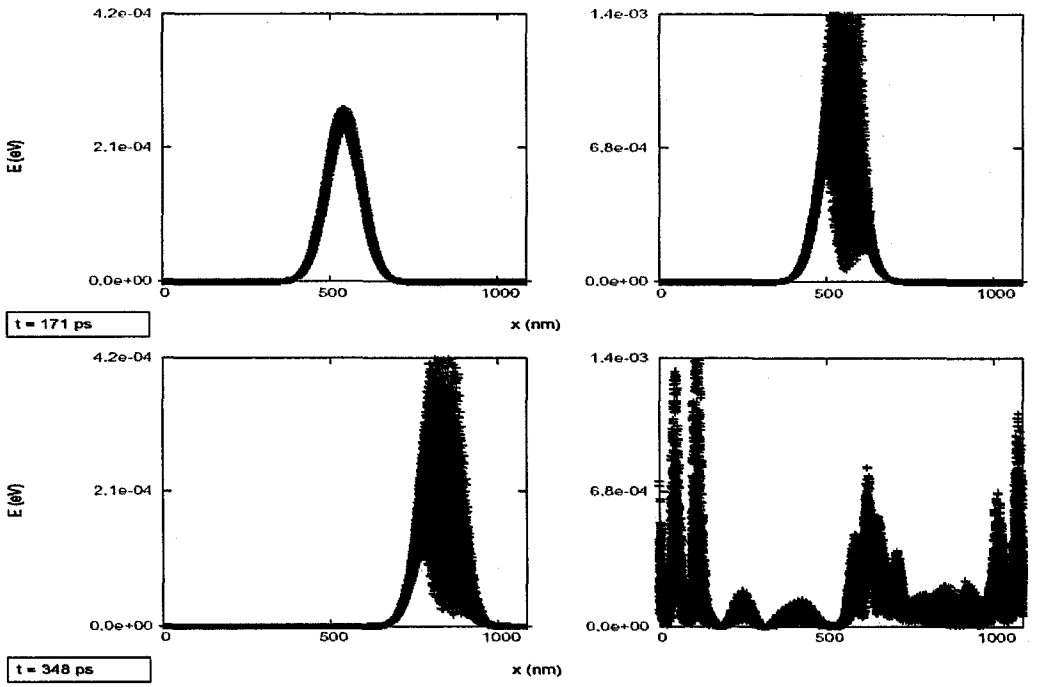

Fig. 6. The evolution of a 4 *eV* hotspot (right) is compared with that of a 1 *eV* hotspot (left). The decay time is roughly proportional to the maximum amplitude (and hence, proportional to the square root of the energy).

We have performed preliminary calculations in this regard by comparing the collapse of hotspots of the same size but with different energy densities. The "decay" times of wavepackets with 1 *eV* and 4 *eV* are found to be approximately 348 *ps* and 171 *ps* as shown in Figure 6. However, these numbers are reported here only to show that it is possible to extract decay rates from the simulation. They are not realistic for the reasons outlined above. To observe actual scattering, we need to turn on or unfreeze the background equilibrium phonons at room temperature. This is expected to be fairly straightforward if the wavepacket can be stabilized against pseudo-scattering in the frozen system. Interpreting the processed data is however, expected to be more intricate due to the presence of the equilibrium phonons.

II.e. Discussion and future work

The present work reveals very detailed phonon physics related to high density phonon sources in transistors. Optical phonon wavepackets corresponding to phonon hotspots are simulated through molecular dynamics. The simulations show that creating a hotspot leads to a local strain which is critical to the stability of the hotspot. Cancellation of this strain leads to the collapse of the whole wavepacket. We find that finite size effects need to be suppressed in these simulations to get physically realistic phonon scattering. This is currently being explored by introducing additional strains in the system that cancel out all strain except that local to the hotspot. Subsequently, by turning on background equilibrium phonons, we expect to see phonon decay and calculate relevant scattering rates. Compact models that utilize these rates to estimate the peak temperature in a device are already in place as noted above. This work is the first exploration of phonon transport in transistors through atomistic simulations and the approach appears very promising in that it provides a very detailed picture of phonon transport at nanoscales with the possibility of extracting unknown scattering rates.

III. Two-fluid Resistance to Heat Conduction from Sub-continuum Optical Phonon Hotspots

III.a. Introduction

The continued scaling of semiconductor devices is yielding devices with gate lengths less than one tenth of a micron, which is comparable to the mean free path of phonons, around 300 nm in silicon [11]. This introduces at least three sub-continuum transport phenomena that effectively reduce heat flow rate from the transistor. The increased thermal resistance serves to lower the electrical conductance of the device and promotes electro-static discharge failures [12]. Modeling of sub-continuum thermal effects is, therefore, helpful in understanding the characteristics of nanotransistors, and critical in improving their reliability. The first thermal phenomenon of interest in the context of transistors is phononboundary scattering, which reduces the thermal conductivity of the constituent thin silicon films. Past research has extensively studied phonon transport in semiconducting thin films (e.g. [4, 11, 13]). An important contribution is a revised estimate of the phonon mean free path in silicon at room temperature, from the gray-body approximation based figure of 43 nm to a semi-empirical figure of 300 nm [11]. A second phenomenon of interest is a geometrical effect related to the sub-continuum size of the heat generation region near the transistor drain.

Monte Carlo as well as continuum device simulations [5, 14–16] show that intense lattice heating by electrons occurs over a length of about 30 - 40 nm along the channel at the drain of silicon transistors. This results in a region of intense phonon generation, or phonon hotspot, as shown schematically in Figure. 7. Chen [14] showed that phonons are emitted ballistically from a spherical hotspot whose size is less than the acoustic phonon mean free path, Λ, leading to a local reduction in thermal conductance. Phonons radiating from a hotspot in a transistor have the same ballistic behavior except that the geometry is cylindrical. The third phenomenon of interest, more directly linked to device scaling, results from the microscopic transfer of energy from electrons to phonons in the transistor channel, which determines the relative non-equilibrium among phonon modes. Under the typically high electric fields in MOSFETs (~ 10^6 V/cm), a larger fraction of the electronic energy is transferred to low velocity optical phonon modes [16], resulting in poorer conduction from the phonon hotspot. This phenomenon is the target of this work. Phonon heat conduction from such hotspots governs the concentration of phonons at the drain-channel interface. The hotspot is bound to influence the drain series resistance in current MOSFETs and may affect the source injection resistance for nanotransistors at the limits of scaling [17].

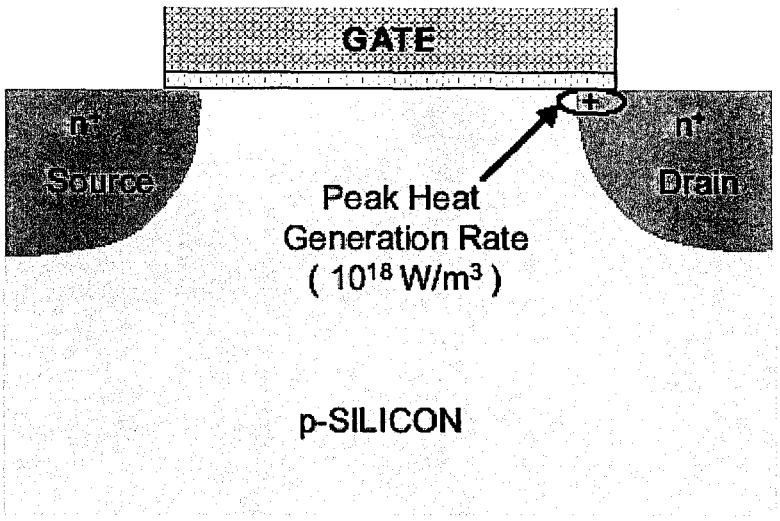

Figure 7: Schematic of a bulk n-MOSFET showing the region of peak heat generation.

The present work develops theory for heat conduction from an electronically generated optical phonon hotspot. The approach is to avoid atomistic or particle based numerical models that are likely to prove computationally prohibitive for device thermal simulations. Instead the model focuses on providing corrections to continuum diffusion theory which is normally used in existing hydrodynamic electron transport models. The analytical subcontinuum thermal model presented here predicts reduced phonon conduction from the nanoscale optical phonon hotspot and is found to compare well with the existing experimental data of Sverdrup et al. [18]. A key challenge of this analysis is the large departure from equilibrium of phonon states within a variety of energy ranges and branches. This is addressed by defining separate temperatures for two groups of phonons, distinguished by their group velocities. This two-fluid approximation for phonons [11, 19] simplifies the phonon dispersion such that energy moments of the Boltzmann equation yield coupled but simplified equations for the two phonon fluids. Another key assumption is the use of a single overall scattering time, which enables the simplification of the collision integral to yield a closed-form thermal resistance between the temperature of phonons transporting heat and an average phonon temperature. This two-fluid resistance is a sub-continuum correction to the resistance calculated from diffusion theory and can be readily incorporated in hydrodynamic models.

III.b. Phonon transport modeling

A phonon hotspot [20–24] refers to a region of strong phonon excitation with nonequilibrium numbers of high frequency phonons, either zone edge acoustic, or as in the present work, optical. A key characteristic of the hotspot is that the nature of phonon propagation from the hotspot, whether ballistic or diffusive, is determined by the excitation conditions: size of the hotspot, duration of the excitation and the energy deposited. Past research has focused on the propagation regimes at liquid Helium temperatures in pure samples, where apart from the excitation conditions, crystalline properties play a major role [21]. In contrast, hotspots in semiconductor devices are produced at room temperatures through electronic relaxation in the drain, where a high field and degenerate doping limit the electron free path to less than 5 nm. The recent experiments of Sverdrup et al. [18] indicated that there is a thermal resistance associated with the

departure from equilibrium in a hotspot that is dominant when the hotspot dimensions are comparable with or less than the phonon mean free path. The present study attempts to explain these observations through a model based on the phonon Boltzmann transport equation (BTE).

We model phonon transport from the hotspot by breaking the phonon BTE into separate balances for each phonon branch. While significant generation occurs almost all across the phonon frequency spectrum [24], a larger fraction of the electronic energy is transferred to optical modes with increasing electric fields since electrons with energies in excess of 50 meV scatter preferentially with longitudinal optical (LO) phonons [16, 25]. In the present work, we assume high electric field conditions of around 10^6 V/cm so that LO phonons are assumed to receive all the energy from electron scattering. At lower fields the equations must be modified to correctly partition energy between acoustic and optical modes. The collision integral includes elastic scattering with impurities, enharmonic non-equilibrium interaction among phonons of different frequencies and polarizations, and electron-LO-phonon coupling. The steady-state Boltzmann equation can be written as:

$$v\cdot\nabla\varphi = -\frac{\varphi(\omega)-\bar{\varphi}}{\tau_{IMP}(\omega)} - \frac{\varphi(\omega)}{\tau_{AN}(\omega)}\int_{\omega'<\omega} P(\omega\rightarrow\omega')d\omega' - \int_{\omega'>\omega}\frac{\varphi(\omega)}{\tau_{AN}(\omega)}P(\omega\rightarrow\omega')d\omega' + \int_{\omega'<\omega}\frac{\varphi(\omega)}{\tau_{AN}(\omega)}P(\omega\rightarrow\omega')d\omega' + \int_{\omega'>\omega}\frac{\varphi(\omega)}{\tau_{AN}(\omega)}P(\omega\rightarrow\omega')d\omega' + S_{e-p} \quad (3)$$

where v is the group velocity, ω is the angular frequency, φ is the number of phonons per unit volume and angular frequency within the specified branch as a function of position, frequency and direction of propagation, and $\bar{\varphi}$ is the average of the number of phonons over all directions. The subscripts, *IMP* and *AN*, denote elastic impurity and enharmonic phonon scattering respectively. The scattering time, τ, is a strong function of frequency of the scattering phonon, and $S_{e\text{-}p}$ is the electron-phonon coupling, and in the present model, is non-zero only for LO phonons. The probability that a phonon with frequency between ω' and $\omega'+d\omega'$ is created in the enharmonic scattering of the phonon of frequency ω is $P(\omega\rightarrow\omega')$ [26]. Selection rules for 3-phonon processes are incorporated in the probability function.

A goal of this study is to estimate the effect of energy exchange between slow-moving optical phonons and fast acoustic phonons at room temperature. Monte-Carlo simulations [27] show τ_{AN} to vary as ω^{-5} and τ_{imp} to vary as ω^{-4} so that the two scattering times have strong frequency dependencies that are not the same. A rigorous solution accounting for frequency dependence is difficult to obtain since semi-empirical scattering rates for hotspot conditions are available only for low temperatures. Equation 1 is instead approximated using a single overall scattering time, τ, for all scattering processes. A further simplification is to use the two-fluid model for phonon heat conduction as originally proposed by Armstrong [19] and adapted for silicon conduction problems by Lai and Majumdar [16] and Ju and Goodson [11]. The phonon reservoir, whose phonons are assumed to be stationary, comprises the longitudinal optical (LO), transverse optical (TO) and transverse acoustic (TA) branches. We now integrate Eq. 3 over all directions so that the first term on the right hand side vanishes. Multiplying by $\hbar\omega$, integrating over frequency, and adding up branches to form the reservoir group, yields

$$0=\frac{1}{\tau}[-\int_{\omega\in TO,LO,TA}\left(\int_{\omega'\in LA;\omega'<\omega}\int_{\Omega}\varphi(\omega)d\Omega P(\omega\rightarrow\omega')d\omega'\right)\hbar\omega d\omega$$
$$-\int_{\omega\in TA}\left(\int_{\omega'\in LA;\omega'<\omega}\int_{\Omega}\varphi(\omega)d\Omega P(\omega\rightarrow\omega')d\omega'\right)\hbar\omega d\omega$$
$$+\int_{\omega\in TO,LO}\left(\int_{\omega'\in LA;\omega'>\omega}\int_{\Omega}\varphi(\omega')d\Omega P(\omega'\rightarrow\omega)d\omega'\right)\hbar\omega d\omega \quad (4)$$
$$+\int_{\omega\in TA}\left(\int_{\omega'\in LA;\omega'>\omega}\int_{\Omega}\varphi(\omega')d\Omega P(\omega'\rightarrow\omega)d\omega'\right)\hbar\omega d\omega]+q'''$$

The longitudinal acoustic (LA) phonons are assumed to form the other group, referred to as propagating phonons, and are accorded a single group velocity, v. It would at first appear that TA phonons should also form a part of the propagating group rather than the reservoir, given the high velocity of long wavelength TA modes. However, past work [11] has shown that heat conduction in silicon is strongly dominated by LA rather than TA modes and hence, they serve more as reservoir modes when compared to LA. A second energy moments of Eq. 3 for the LA phonons gives the energy equation for the propagating group,

$$v\cdot\nabla\int_{\omega\in LA}\int_{\Omega}\varphi d\Omega\omega d\omega=\frac{1}{\tau}[-\int_{\omega\in LA}\left(\int_{\omega'\in TO,LO,TA;\omega'>\omega}\int_{\Omega}\varphi(\omega)d\Omega P(\omega\rightarrow\omega')d\omega'\right)\omega d\omega$$
$$-\int_{\omega\in LA}\left(\int_{\omega'\in TA;\omega'<\omega}\int_{\Omega}\varphi(\omega)d\Omega P(\omega\rightarrow\omega')d\omega'\right)\omega d\omega$$
$$+\int_{\omega\in LA}\left(\int_{\omega'\in LO,TO,TA;\omega'>\omega}\int_{\Omega}\varphi(\omega')d\Omega P(\omega'\rightarrow\omega)d\omega'\right)\omega d\omega \quad (5)$$
$$+\int_{\omega\in LA}\left(\int_{\omega'\in TA;\omega'<\omega}\int_{\Omega}\varphi(\omega')d\Omega P(\omega'\rightarrow\omega)d\omega'\right)\omega d\omega]$$

We further simplify Eq. 4 by lumping the energy exchange integrals as

$$0 = -\frac{\Delta u_{LR}}{\tau}+q'''=-\frac{C_R(T_R-T_L)}{\tau}+q''' \quad (6)$$

where Δu_{LR} is the energy transferred out of the phonon reservoir at a temperature T_R as it relaxes towards equilibrium with the lattice at the average temperature T_L, q''' is the power generated by hot electrons per unit volume, and C_R is the heat capacity of the reservoir group. Other terms in the summation associated with energy exchange among the LO, TO and TA phonons drop out from a simple energy balance. Equation 5 for the propagating group collapses to

$$\nabla\cdot j_p = -\frac{\Delta u_{PL}}{\tau}=-\frac{C_R(T_L-T_P)}{\tau} \quad (7)$$

where j_P is the heat flux and Δu_{PL} is the energy gained by the propagating phonons, at a temperature T_P , from the phonon reservoir while cooling the lattice. An energy balance on the entire phonon population in the lattice yields

$$(C_P + C_R)(T_L - T_\infty) = C_P (T_P - T_\infty) + C_R (T_R - T_\infty) \quad (8)$$

Equations 6 and 8 are combined to yield an expression for the difference in lattice temperature, T_L, and the temperature of the propagating group (responsible for heat conduction), T_P . The maximum value is

$$(T_L - T_P)_{\max} = \left(\frac{q'''\tau}{C_p}\right)_{\max} = \frac{q'''_{\max}\tau}{C_p} \tag{9}$$

This can be further expressed as a thermal resistance between temperature potentials, T_L and T_P, as

$$R_{LP} = \frac{(T_L - T_P)_{\max}}{q} = \frac{\tau}{q/q'''_{\max} C_P} = \frac{\tau}{V_{effec} C_P} = \frac{\Lambda^2}{3K_{bulk} V_{effec}} \tag{10}$$

The effective volume, V_{effec}, is that of the hotspot, and q is the total power. The resistance for heat transfer from the phonon reservoir to the lattice is

$$R_{RL} = \frac{(T_R - T_L)_{\max}}{q} = \frac{\tau}{q/q'''_{\max} C_R} = \frac{\tau}{V_{effec} C_R} = \frac{\Lambda^2}{3K_{bulk} V_{effec}}\left(\frac{C_P}{C_R}\right) \tag{11}$$

Figure 8 shows the effective thermal resistances in the two-fluid model. The heat capacity of the propagating phonons is approximately 25% of the heat capacity of the phonon reservoir over a long range of temperature. The lattice to phonon-reservoir resistance is thus about 25% of the lattice to propagating-phonon resistance. Equation 8 is the resistance to heat conduction, rather than Eq. 11, because Eq. 10 sustains the difference between the mean phonon temperature and the temperature of phonons conducting heat away from the hotspot.

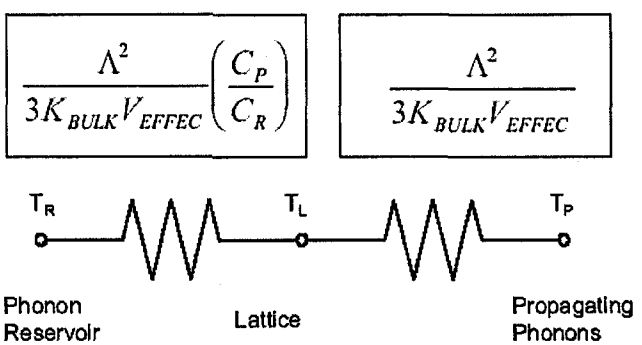

Figure 8: The two-fluid resistance is the thermal resistance between the lattice temperature (or mean phonon temperature) and the temperature of propagating phonons, which conduct heat from the hotspot.

The largest possible impact of the two-step energy transfer can be estimated by considering a spherical hotspot of radius r in an infinite medium. The ratio of the thermal resistance in Eq. 10 to the thermal resistance based on the continuum heat diffusion equation and the Fourier law,

$$\frac{R_{LP}}{R_{DIFF}} = \frac{\Lambda^2/4\pi r^3 K}{1/4\pi r K} = \left(\frac{\Lambda}{r}\right)^2 \tag{12}$$

III.c. Comparison of Thermal Resistance Predictions with data for ballistic transport

III.c.1. Measurement of ballistic conduction near a hotspot

This section reviews a previous set of measurements that probed ballistic phonon conduction [18] and are useful for comparison with the model developed here. The experiments used heating in a doped resistor-thermometer in silicon, shown in Figure 9, which approximated the much smaller phonon source in a transistor. To induce ballistic transport using the large source, the measurements were performed at 100-200 K where the phonon 10 mean free path ranges between 2 and 10 mm. The p-type resistor was fabricated using boron implantation in a silicon-on-insulator (SOI) film. The effect of implant damage on thermal conductivity of the resistor was shown to be negligible. The membrane geometry, which reduced experimental uncertainty, was formed by plasma etching the underlying silicon. The structure was mounted in a cryostat to maintain a constant temperature vacuum environment. The p-n junction between the resistor and the substrate was reverse biased to confine the current along the resistor.

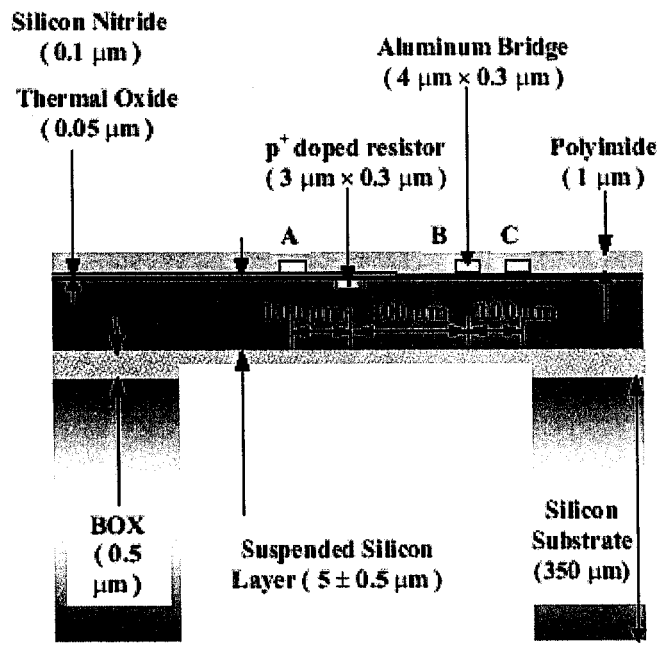

Figure 9: Cross-section of the experimental structure used to probe ballistic conduction near a doped resistor in silicon [18]. The resistor acted as a hotspot inside the silicon membrane.

Joule heating in the doped resistor induces a temperature rise in the membrane structure. The thermal conductivity and mean free path in the silicon membrane were determined from the temperature rises of the parallel aluminum bridges A, B, and C, which served as electrical resistance thermometers. Ballistic phonon transport was observed through the departure of the doped resistor temperature from predictions based on the Fourier law.

III.c.2. Results and discussion

Figure 10 shows a comparison of the membrane thermal resistance measured by Sverdrup et al. [18] at different base temperatures with predictions of the resistance using the two-fluid resistance of Eq. 10. The dashed line shows the thermal resistance of the membrane structure calculated from diffusion theory using the bulk thermal conductivity of silicon. Phonon boundary scattering reduces the thermal conductivity of the membrane. The dotted line is the thermal resistance calculated from diffusion theory but using the thermal conductivity of the membrane measured in situ. The measurements increasingly differ from predictions of diffusion theory as the temperature decreases and the mean free path becomes longer. This is attributed to ballistic phonon transport near the doped resistor. The relative increase in thermal resistance varies between 56% at 100 K, where the mean free path is approximately 10 mm, to less than 1% at 290 K, where the phonon mean free path is approximately 300 nm.

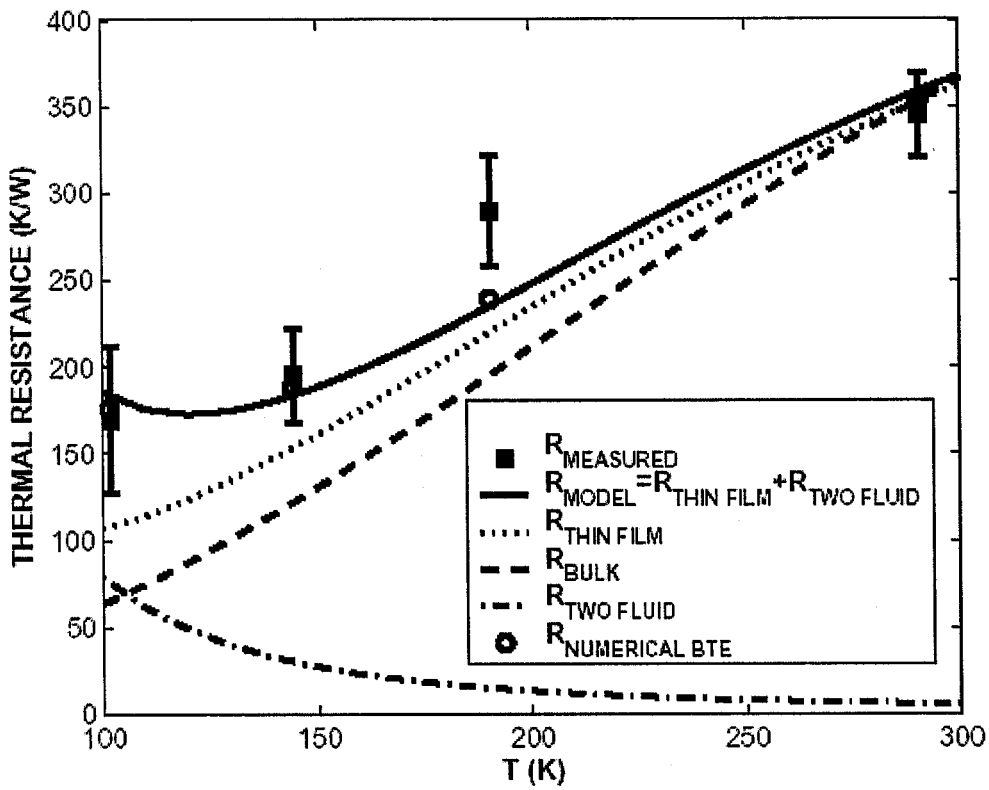

Figure 10: A comparison of the thermal resistance measured at different temperatures. The analytical two-fluid model is in close agreement with a numerical solution to the two-fluid phonon BTE [5] and thermometry data for hotspots [18].

The solid line represents the sum total of the two-fluid resistance of Eq. 10 and the diffusion resistance depicted by the dotted line. The closed-form two-fluid prediction agrees well with a full numerical solution to the Boltzmann transport equation applied to a two- fluid phonon system [18]. Both predictions are consistent with the data at 100 and 140 K, where the departure from diffusion theory is substantial. The data at 190 K exceed the predictions substantially, and represent a large departure from any existing theory for reasons that remain unclear.

Figure 11 compares the thermal resistance of ballistic phonon transport near a spherical hotspot in bulk silicon, derived by Chen [14], with the two-fluid resistance, given by Eq. 10. Chen's derivation accounts for geometry related effects which are missing in the two-fluid model. An overall effect can be estimated by assuming the resistances to be acting in series to impede heat conduction from the hotspot. The two-fluid resistance provides the impedance due to strong excitation of a stationary phonon mode and the ballistic resistance provides the impedance due to emission of propagating phonons from the hotspot. The two-fluid resistance is found to be larger than the resistance due to ballistic emission by a factor of more than 20 for a hotspot of radius 10 nm at room temperature. This is partly due to the severe assumption about the nature of phonon excitation inherent in the two-fluid model. The cumulative resistance is about 850 times larger than the resistance calculated from the diffusion theory. This factor decreases to around 30 as temperature in the bulk increases from 300 K to 1000 K.

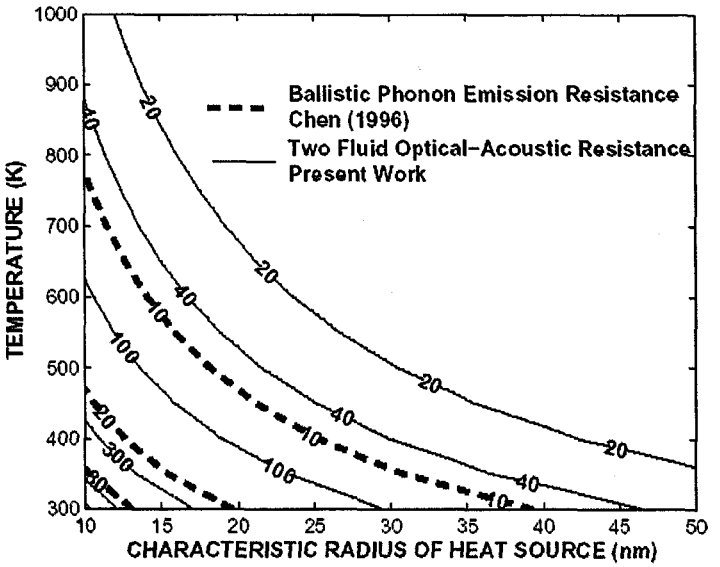

Figure 11: A comparison of the thermal resistance of ballistic phonon emission with the two-fluid resistance of Eq. 10.

III.d. Conclusion

It has already been well established by past work that the temperature rise in modern semiconductor devices is poorly predicted by the heat diffusion equation based on Fourier's law. This work refines the theory for the conduction problem within sub-micrometer transistors by modeling the impact of strong excitation of low velocity optical phonon modes. The resulting two-fluid thermal resistance is important when the hotspot is small compared to the acoustic phonon mean free path. The resistance serves as a correction term for predicting the temperature rise in a transistor using continuum diffusion theory. Future work needs to consider the frequency dependence of the phonon generation. The development presented in this work can then be modified to treat phonon generation across all modes and obtain a more precise picture of phonon transport at the hotspot. The transient problem is also of considerable interest since the time constant for heat dissipation from the hotspot, which is the enharmonic lifetime of LO phonons is approximately 5 ps for silicon at room temperature whereas device switching times are already approaching 100 ps. Energy accumulation at the hotspot becomes significant for such

semiconductor devices. The two-fluid model developed here is intended as a starting point for exploring the problem of phonon transport in nanotransistors where sub-continuum phenomena will be stronger due to reduced dimensions. Additional experimental data is needed to provide more physical insight as to the size scale effect of heat sources on temperature localization. With the use of techniques such electron beam or EUV lithography, the creation of new test structures to explore these length scale effects should be feasible.

References

[1] P. Sverdrup, S. Sinha, M. Asheghi, S. Uma and K.E. Goodson, "Measurement of ballistic phonon conduction near hotspots in silicon", Appl. Phys. Lett., v. 78, pp. 3331-3333, May 2001.
[2] S. Sinha and K.E. Goodson, "Phonon Heat Conduction from nanoscale Hotspots in Semiconductors", Proc. Twelfth Int. Heat Transfer Conf., pp. 573-578, Grenoble, France, Aug. 2002.
[3] E. Pop, K. Banerjee, P. Sverdrup, R. Dutton, K. Goodson, "Localized Heating Effects and Scaling of Sub-0.18 Micron CMOS Devices", Proc. Int. Electron Devices Meeting, Dec. 2001, Washington DC.
[4] S. Mazumder and A. Majumdar, "Monte Carlo Study of Phonon Transport in Solid Thin Films Including Dispersion and Polarization", J. Heat Transfer, v. 123, pp. 749-759, Aug. 2001.
[5] P. Sverdrup, Y.S. Ju and K.E. Goodson, "Sub-continuum simulations of heat conduction in silicon-on-insulator transistors", J. Heat Transfer, v. 123, pp. 130-137, Feb. 2001.
[6] A.A. Maradudin and A.E. Fein, "Scattering of Neutrons by an Enharmonic Crystal", Phys. Rev., v. 128, pp. 2589-2608, Dec. 1962.
[7] M.G. Holland,"Analysis of Lattice Thermal Conductivity", Phys. Rev., v. 132, pp. 2461-2471, Dec. 1963.
[8] J. Shah, "Ultrafast Spectroscopy Of Semiconductors And Semiconductor Nanostructures", Springer-Verlag, 1996.
[9] D. Long, "Scattering of conduction electrons by lattice vibrations in silicon", Phys. Rev., vol. 120, pp. 2024-2032, Dec. 1960.
[10] F.H. Stillinger and T.A. Weber, "Computer Simulation of Local Order in Condensed Phases of Silicon", Phys. Rev. B, v. 31, pp. 5262-5271, Apr. 1985.
[11] Y. Ju and K. Goodson, Appl. Phys. Lett. 74, 3005 (1999).
[12] A. Amerasekera and C. Duvvury, *ESD in Silicon Integrated Circuits* (John Wiley & Sons, Ltd., England, 2002).
[13] M. Asheghi, M. Touzelbaev, K. Goodson, Y. Leung, and S. Wong, J. Heat Transfer 120, 30 (1998).
[14] G. Chen, J. Heat Transfer 118, 539 (1996).
[15] E. Pop, R. W. Dutton, and K. Goodson, in *Proc. SISPAD (IEEE)* (Boston, 2003).
[16] J. Lai and A. Majumdar, J. Appl. Phys. 79, 7353 (1996).
[17] E. Pop, K. Bannerjee, P. Sverdrup, R. W. Dutton, and K. Goodson, in *Proc. International Electron Devices Meeting (IEDM)* (Washington D.C., 2001).
[18] P. Sverdrup, S. Sinha, M. Asheghi, U. Srinivasan, and K. Goodson, Appl. Phys. Lett. 78, 3331 (2001b).
[19] B. H. Armstrong, Phys. Rev. B 23, 883 (1981).
[20] J. Hensel and R. Dynes, Phys. Rev. Lett. 39, 969 (1977).
[21] J. Shields and J. Wolfe, Z. Phys. B 75, 11 (1989).
[22] J. Shields, M. Msall, M. Carroll, and J. Wolfe, Phys. Rev. B 47, 12510 (1993).
[23] D. Kazakovtsev and I. Levinson, Sov. Phys. JETP 61, 1318 (1985).
[24] H. J. Maris and S. ichiro Tamura, Phys. Rev. B 47, 727 (1993).
[25] C. Jacoboni and L. Reggiani, Rev. Mod. Phys. 55, 645 (1983).
[26] H. J. Maris, Phys. Rev. B 41, 9736 (1990).
[27] S. Ichiro Tamura, Phys. Rev. B 48, 502 (1993).

Distribution List

1 MS 0102 J.B. Woodard, 00002
1 MS 0825 W.L. Hermina, 9110
1 MS 0826 S.N. Kempka, 9113
1 MS 0834 M.R. Prairie, 9112

1 MS 9001 M.E. John, 08000
1 MS 9403 J.M. Hruby, 08700
Attn: MS 9042 C.D. Moen, 8752
MS 9161 D. Medlin, 8761
MS 9401 G.F. Cardinale, 08753
MS-9042 P.A. Spence, 8774
MS-9401 J. E Goldsmith, 8751
MS 9403 T.J. Shepodd, 8762
MS 8763 T. Chen, 8763
MS 9402 C.H. Cadden, 8772
MS 9402 J. Wang, 8773

1 MS9404 G.D. Kubiak, 08750
1 MS9405 K.L. Wilson, 08770
5 MS9409 J.R. Garcia, 08754

Samuel Graham
Woodruff School of Mechanical Engineering
Georgia Institute of Technology
771 Ferst Dr.
Atlanta, GA 30332-0405

Sanjiv Sinha
Stanford University
2575 Sand Hill Road
Menlo Park, CA 94025

Kenneth Goodson
Stanford University
2575 Sand Hill Road
Menlo Park, CA 94025

3 MS 9018 Central Technical Files, 8945-1
1 MS 0899 Technical Library, 9616
1 MS 9021 Classification Office, 8511 for Technical Library,
1 MS 0899, 9616 DOE/OSTI via URL
1 MS 0323 D. Chavez, LDRD Office, 1011

This Page Left Intentionally Blank